Journal of Cleaner Production 268 (2020) 121575

Contents lists available at ScienceDirect

Journal of Cleaner Production

journal homepage: www.elsevier.com/locate/jclepro

Revisiting the environmental Kuznets curve for city-level CO_2 emissions: based on corrected NPP-VIIRS nighttime light data in China

Hongxing Chen [a, b], Xiaoling Zhang [c, d, *], Rongwei Wu [a, b, **], Tianyi Cai [a, b]

[a] State Key Laboratory of Desert and Oasis Ecology, Xinjiang Institute of Ecology and Geography, Chinese Academy of Sciences, Urumqi, 830011, China
[b] University of Chinese Academy of Sciences, Beijing, 100049, China
[c] Department of Public Policy, City University of Hong Kong, Hong Kong, China
[d] Shenzhen Research Institute, City University of Hong Kong, Shenzhen, 518057, China

ARTICLE INFO

Article history:
Received 16 November 2019
Received in revised form
6 April 2020
Accepted 6 April 2020
Available online 12 May 2020

Handling editor: Cecilia Maria Villas Bôas de Almeida

Keywords:
Corrected NPP-VIIRS data
CO_2 emissions
City level
Environmental Kuznets curve (EKC)
Spatial econometric model
China

ABSTRACT

With the increasing trend of global warming, the Chinese government faces tremendous pressure to reduce CO_2 emissions. The purpose of this study is to accurately measure CO_2 emissions at the city scale in China and examine the environmental Kuznets curve, thereby providing a reference for decision-making. Corrected NPP-VIIRS nighttime light data were used to accurately estimate carbon dioxide emissions at the provincial and city scales in China. Then, based on the STRIPAT model, 291 cities in China were used to verify the environmental Kuznets curve. Our results show that on the provincial scale, the R^2 between the estimated value and the statistical value of carbon dioxide reaches 0.85. Western cities in China emit more CO_2, as do economically developed cities and industry- and mining-dominated cities. There are two CO_2 emission hot spots in the north and one cold spot in the south. It was found that the environmental Kuznets curve on the city scale exists. This study has practical value in utilizing NPP-VIIRS data for the estimation of city CO_2 emissions. The results also have academic value for determining factors that contribute to carbon dioxide emissions and can provide a reference for relevant decision makers. This study could be considered the first to simulate CO_2 emissions at the provincial and city levels in China based on a NPP-VIIRS nighttime light model to explore the associated geographical distribution characteristics and potential influencing factors.

1. Introduction

Issues related to climate change have attracted much attention worldwide and have become an increasingly pressing problem facing society (Fan et al., 2016; Nicholson-Cole, 2005). Global warming is one of the most serious current events, which has affected human beings socially, politically, and economically in recent decades (Ang, 2009; Lu et al., 2007). Reports from the Intergovernmental Panel on Climate Change (IPCC) and other studies show that carbon dioxide (CO_2) emissions are the most important contributor (Griggs and Noguer, 2010; Karl and Trenberth, 2003) to global warming. Human activities have greatly exacerbated the process of climate warming and caused many adverse effects on the natural ecological environment on the earth's surface. The Paris Agreement proposes that in the 21st century, the world should strive to control the increase of the global average temperature to below 2 °C higher than that in the pre-industrial era, preferably reaching below 1.5 °C. As the temperature increase is triggered by the accumulation of greenhouse gases (GHGs), this global problem requires the cooperation of all countries and groups. As of 2016, a total of 178 parties had signed the Paris Agreement. Most countries have made commitments to curb global warming caused by harmful emissions from burning coal, oil and natural gas. China became the 23rd party to complete the ratification agreement. As the world's second largest economy and the largest greenhouse gas emitter (Guan et al., 2014; Mu et al., 2013), China needs to take appropriate responsibility for reducing its CO_2 emissions to curb the trend of accelerated global warming. In 2016, China announced that its total emissions will peak by the year 2030 (Li et al., 2018).

* Corresponding author. Department of Public Policy, City University of Hong Kong, Hong Kong, China.
** Corresponding author. State Key Laboratory of Desert and Oasis Ecology, Xinjiang Institute of Ecology and Geography, Chinese Academy of Sciences, Urumqi, 830011, China.
E-mail addresses: xiaoling.zhang@cityu.edu.hk (X. Zhang), wurongwei16@mails.ucas.ac.cn (R. Wu).

https://doi.org/10.1016/j.jclepro.2020.121575
0959-6526/

However, the annual average growth rate of CO_2 emissions in China has reached approximately 10% since 2000 (Liu et al., 2010). Additionally, China contributes 27.3% to the world's energy-related CO_2 emissions (Jiang et al., 2018). According to the Global Carbon Budget Report (2017), China's CO_2 emissions were nearly twice those of the United States in 2016. Facing huge pressure to reduce CO_2 emissions, the Chinese government had to implement a crucial national emissions reduction strategy in its 12th five-year plan, committing to reducing its intensity of CO_2 emissions (calculated as CO_2 per unit of GDP) by 17% between 2011 and 2015. In addition, the Chinese government promised in a joint statement with the United States in 2014 that its national CO_2 emissions would peak by 2030 and then decline (Wang and Liu, 2017). To reach the CO_2 emissions reduction target as soon as possible, the Chinese government needs detailed CO_2 emissions data to accurately implement different countermeasures for different cities. The statistical scale of CO_2 emissions from energy consumption is limited to the provincial level at present. Measuring CO_2 emissions at a finer scale is a key step in achieving emissions reduction targets. China has experienced rapid urbanization, with an increase from 16.4% of the population living in urban areas in 1949 to 58.52% in 2017 (Zhou et al., 2020). The 35 largest cities contribute 40% of China's CO_2 emissions (Ouyang and Lin, 2017). Therefore, a current problem facing academia and politicians involves measuring the level of CO_2 emissions in various cities accurately and efficiently. In recent years, nighttime light (NTL) data have become a powerful tool for measuring carbon dioxide emissions. Many scholars have performed studies on carbon dioxide emissions using nighttime light data, including the Defense Meteorological Satellite Program's Operational Linescan System (DMSP-OLS) NTL data and the Suomi National Polar-orbiting Partnership-Visible Infrared Imaging Radiometer Suite (NPP-VIIRS) NTL data (Lv et al., 2020).

In this study, we apply corrected nighttime light data to estimate the CO_2 emissions of China at the city level. This corrected method was first proposed by Ghosh et al. (2010), and Ou et al. (2015) used it to map CO_2 emissions worldwide, applying scatter plots to fit the statistics and simulations using the 50 U.S. states. The resulting R^2 of above 0.8 showed that NPP-VIIRS can be a powerful tool for use in studying CO_2 distributions. However, previous authors did not consider the practicability of this method in China, and there is a lack of in-depth analysis of the potential socio-economic factors affecting CO_2 emissions at the city level.

The contribution of this research is mainly embodied on the following aspects. In terms of research content, we used the corrected NPP-VIIRS NTL data to estimate carbon dioxide emissions from energy consumption in 30 provinces and 291 cities in China for the first time. In addition, we carried out the visualization and hot spot analysis of urban per capita CO_2 emissions, and high-emission zones and hot and cold regions are presented on a map. Based on these data, the environmental Kuznets curve was tested based on the STRIPT model. In terms of maintaining regional sustainable development, energy conservation and emissions reduction, the inflection point of the Kuznets curve was predicted. Through further analysis of the influencing factors of city development such as the per capita GDP, FAI, urbanization rate, etc., development recommendations and countermeasures are proposed for certain cities order to control the total CO_2 emissions and reduce per capita CO_2 emissions.

2. Literature review

In recent decades, many studies have sought to measure China's carbon emissions at different geographical scales and by different methods. The province and the city are often used as the basic study unit (Shan et al., 2016). The various methods used to measure carbon emissions include constructing carbon inventories (Shan et al., 2018), modeling the carbon footprint (Brown et al., 2009), and input-output analysis (Shao et al., 2016). In addition, some scholars use data from unofficial sectors to explore carbon dioxide emissions measurements. Based on data from enterprises, Cai established a set of bottom-up methods to build China's high-resolution emissions database and provided statistics on carbon dioxide emissions at the city scale (Cai et al., 2018b). Based on questionnaire survey data, the basic conditions and influencing factors of household CO_2 emissions in Northwest China were measured by Li et al. (2016).The consensus is that the total carbon emissions in eastern China are higher than those in western or central China (Zhou and Wang, 2018). In the industrial sector, energy supply sectors such as oil and gas extraction and non-ferrous ore extraction and processing are among the highest carbon emitters (Li et al.,2020).

Although some progress has been made in the study of CO_2 emissions at the provincial level (Kang et al., 2012; Wang et al., 2014), the accurate implementation of a carbon emissions policy requires the simulation of carbon emissions at more detailed scales, such as the city scale. Qiao et al. proposed a top-to-bottom approach, selecting 41 cities in the eastern, central, and western regions of China and analyzing the uncertainty of the spatial differentiation of energy consumption and the influencing factors of fossil fuel emissions (Jing et al., 2018). Cai systematically analyzed the driving forces behind carbon dioxide emissions in 286 prefecture-level cities in 2012 and confirmed the impact of the economic scale and structure on China's urban carbon dioxide emissions through regression analysis (Cai et al., 2018a). Cui took 16 cities in Xinjiang as examples, measured the carbon emissions from energy consumption, and analyzed the influencing factors leading to the growth of carbon dioxide emissions in each city (Cui et al., 2019). However, energy consumption data at the city level are available in the statistical yearbooks of only a few cities, so the existing literature relating to city carbon emissions is quite limited (Wang and Liu, 2017). This constraint restricts the overall understanding of CO_2 emissions below the provincial level. In addition, differences in the statistical quality of national-, provincial-, and municipal-level data lead to estimation errors, making it difficult to formulate accurate, systematic, and differentiated carbon emissions reduction plans.

Many scholars have applied nighttime light data as a useful proxy to intuitively reflect the intensity of urban human activities, and this method has the advantage of being convenient, inexpensive, and objective (Wu et al., 2018a). Some studies have successfully applied NTL data to such issues as monitoring urban expansion (Chai et al., 2016; Liu et al., 2012; Ouyang et al., 2016); examining the urbanization process (Yi et al., 2014); and estimating socio-economic factors (Li et al., 2013), energy consumption (Wang and Liu, 2017), and nitrogen oxide emissions (Jiang et al., 2016).

Previous research has demonstrated that NTL data obtained from the DMSP-OLS NTL data have a relatively strong correlation with CO_2 emissions when used to estimate city-level emissions (Shi et al., 2016). Using a panel analysis method, Shi et al. examined the utility of DMSP-OLS NTL data in simulating the spatiotemporal distribution of carbon dioxide (Shi et al., 2016). Based on three datasets including DMSP-OLS NTL data, population density maps, and an energy balance table, by utilizing the top-down method, Meng et al. estimated CO_2 emissions at the urban scale and concluded that the share of CO_2 emissions from urban areas increases continuously (Meng et al., 2014). Although useful, DMSP-OLS NTL data have limitations, such as a relatively low spatial resolution, blooming (the "spilling" of nightlight from urban areas into dark areas), and the internal calibration of sensors (Elvidge et al., 2010; Ou et al., 2015). Compared with

DMSP-OLS NTL data, the spatial resolution of the NPP-VIIRS NTL data (15 arc seconds, approximately 500 m) is relatively high, which increases the accuracy of associated assessments. In addition, DMSP data have not been updated after 2013 and thus cannot be used to estimate CO_2 emissions after that time. Ou et al. (2015) proposed a new correction approach for estimating carbon emissions in 2012, which combines the population grid and NTL data. Their approach is more accurate and reliable compared to the simple use of digital number values to fit carbon emissions. The carbon emissions values obtained by the modified method have been shown to have high statistical value. Moreover, NPP-VIIRS data are more advantageous than DMSP-OLS data when this method is applied.

In addition to facilitating the decomposition of the mitigation target, city-level CO_2 emission data help in examining the relationship between economic growth and CO_2 emissions (Chen et al., 2019; He et al., 2014; Wang and Ye, 2017). The environmental Kuznets curve (EKC) hypothesis has been widely tested to explore whether a traditional inverted U-shaped curve exists between the wealth level and pollutants (Kang et al., 2016). However, the reasons behind increases or decreases in CO_2 are extremely complex. Therefore, empirical studies have been employed to observe the inverted U-shaped relationship (Zhao et al., 2016), as well as inverted N-shaped (Wu et al., 2018b), and N-shaped relationships (Ozokcu and Ozdemir, 2017). Some scholars consider that the relationship between CO_2 emissions and the economic level does not satisfy the EKC hypothesis (Wang and Ye, 2017). These divergent conclusions are due to the use of different datasets and observations over different time periods. Additionally, in exploring the relationship between economic growth and CO_2 emissions, other potential influencing factors have been incorporated into the analytical framework. Generally, in addition to index decomposition analysis (Yao et al., 2015) and the input-output model (Zhu et al., 2012), the IPAT model and its expanded form, the STIRPAT model, have been widely utilized to explore the factors contributing to carbon emissions (Cui et al., 2019). For instance, based on the extended STIRPAT model, Wang et al. (2013) examined the factors influencing energy-related CO_2 emissions in Guangdong Province, finding the population, economic growth, and industrial structure to be the main causes of increasing carbon emissions. Cheng et al. (2013) found the energy structure, industrial structure, and urbanization rate to be important in the evolution of the carbon emissions intensity pattern. Additionally, using Tianjin as an example, Li et al. (2015) found that urbanization is the greatest factor boosting CO_2 emissions, with the level of affluence, population size, and foreign direct investment (FDI) also contributing. There is therefore a variety of causes of CO_2 emissions.

3. Materials and method

3.1. Study area

The study area is mainland China, and considering the availability of data, 30 provinces and 291 cities comprise the research sample.

3.2. Data collection

The main data comprise 2015 and 2016 NPP-VIIRS nighttime composites, a China population spatial distribution kilometer grid dataset, energy consumption statistical data, data on socioeconomic indicators (including the GDP per capita, industrial structure, urbanization rate, January temperature, investment in fixed assets, expenditure on science and technology, and foreign capital utilization), and basic geographic information data at the national level (mainly administrative boundary data). The NPP-VIIRS nighttime data are from the NOAA/NGDC website (https://ngdc.noaa.gov/eog/viirs/download_dnb_composites.html), the Chinese population spatial distribution kilometer grid dataset is from the Resource and Environment Data Cloud Platform (Xu, 2017), and the provincial-level fossil energy consumption data and the above-mentioned indicator data are derived from the 2016 and 2017 national and relevant cities' statistical yearbooks.

3.3. Methods

3.3.1. Measuring provincial CO_2 emissions from energy consumption

While most previous studies calculated the CO_2 emissions of China using the method provided by the IPCC (Ma et al., 2019; Zhang et al., 2019), this study estimates the CO_2 emissions from energy consumption by

$$CO_2 = \frac{44}{12} \times \sum_{i=1}^{8} K_i E_i \quad (1)$$

where K_i represents the carbon emission factor of the ith type of energy and i represents 8 types of energy, comprising raw coal, coke, crude oil, gasoline, kerosene, diesel, fuel oil, and natural gas. $E_i$is the consumption of the ith type of energy, which should be converted to standard coal equivalents, and $\frac{44}{12}$ is the molar ratio of CO_2 to C.

3.3.2. Mapping emissions with corrected NTL data for both provinces and cities

A top-down methodology is used to convert CO_2 emissions at large geographic scales to finer research units based on the NPP-VIIRS NTL and population grid data. In this model, we use different methods to allocate the carbon dioxide emissions for the bright areas (where light radiation can be detected) and dark areas (where light radiation cannot be detected). For the former, CO_2 emissions are distributed in proportion to the radiation value of the NTL data. For the latter, previous studies showed population data to be a useful proxy for detecting the CO_2 emissions of dark grids (Elvidge et al., 2011), so population grid data were used to measure corresponding emissions. In this model, following Ghosh et al. (2010) and Ou et al. (2015), it is assumed that the per capita CO_2 emissions in dark areas are half of those in bright areas. Based on this background, the detailed calculation process is as follows:

(1) First, we assume that the per capita CO_2 emissions in the light and dark areas of administrative unit j are x_j and$x_j/2$, respectively. Notably, the 1/2 factor is mentioned by Ou et al. (2015), who suggest that the lack of a better recognized value makes this ratio an uncertain parameter in measuring the relationship between CO_2 emissions per capita from light and dark areas. However, as in Ou's study, the use of this parameter leads to better simulation results for estimating carbon emissions. This finding shows the usefulness of this parameter and promotes its further testing and discussion in future research.

Based on ArcGIS10.2, the sum of the population data of the light areas in administrative unit $j(SP_{Lj})$is extracted by the China NTL mask. In the same way, the sum of the population data of the dark areas in administrative unit $j(SP_{Dj})$is extracted by the China NTL mask. The total CO_2 emissions of light and dark areas in administrative unit $j(CO_{2Lj}, CO_{2Dj})$are calculated using

$$CO_{2Lj} = SP_{Lj} * x_j \quad (2)$$

$$CO_{2Dj} = SP_{Dj} * (x_j / 2) \quad (3)$$

According to Eq. (2) and Eq. (3), the per capita CO_2 emissions of unit $j(x_j)$ in light areas are given by

$$x_j = TCO_{2j} / (SP_{Lj} + SP_{Dj} / 2) \quad (4)$$

The carbon emissions in light and dark areas constitute the total CO_2 emissions of administrative unit $j(TCO_{2j})$, as follows

$$TCO_{2j} = CO_{2Lj} + CO_{2Dj} \quad (5)$$

(2) To obtain the CO_2 emissions of the light grid of administrative unit $j(CO_{2Lgj})$, first, the CO_2 emissions per radiance are calculated as being equal to the ratio of the total CO_2 emissions of light areas of administrative unit $j(CO_{2Lj})$ and the total light value of administrative unit $j(TL_j)$. Then, each light grid's radiation value in administrative unit $j(L_{gj})$ is multiplied by the ratio described above. Thus, the light areas' CO_2 emissions grid value of the of the administrative unit $j(CO_{2Lgj})$is acquired by

$$CO_{2Lgj} = L_{gj} * (CO_{2Lj} / TL_j) \quad (6)$$

Similarly, for dark areas, the per capita CO_2 emissions are equal to the ratio of the dark areas' total CO_2 emissions in administrative unit j (CO_{2Dj}) to the sum of corresponding population of administrative unit j (SP_{Dj}). Therefore, dark areas' CO_2 emissions in administrative unit j (CO_{2Dgj}) equal the product of the per capita CO_2 emissions (the ratio given above) and the population count in each grid of the dark areas in administrative unit j (P_{Dgj}). The formula is as follows

$$CO_{2Dgj} = P_{Dgj} * (CO_{2Dj} / SP_{Dj}) \quad (7)$$

(3) According to Eqs. (5) and (6), the total CO_2 emissions of administrative unit j (CO_{2j}) are equal to the sum of the light areas' CO_2 emissions(CO_{2Lgj}) and the dark areas' CO_2 emissions (CO_{2Dgj}) in administrative unit j, where

$$CO_{2j} = \sum_{g=1}^{N} CO_{2Lgj} + \sum_{g=1}^{M} CO_{2Dgj} \quad (8)$$

Following the above method, the CO_2 emissions of provincial administrative units are estimated using the corrected NTL. Then, we establish the correlation between the estimated value and the statistical CO_2 emissions. Additionally, we check the fitting accuracy to verify the applicability of the estimation method, and the correlation shows a significant linear relationship between the estimates and statistics. The final step is to estimate the CO_2 emissions of each city through an inversion strategy. Specifically, first, through Eqs. (2)–(7), we obtain the carbon dioxide emissions of each grid. Then, using the district statistics tool from ArcGIS 10.2, we determine the carbon dioxide value of each city. Third, through the linear relationship described above, we model China's national city-level CO_2 emissions.

3.3.3. Examination of the EKC at the city level in China

The relationships between the CO_2 emissions and per capita income and the EKC have been widely discussed in environmental economics (e.g., Omri et al., 2019). The extended form of the traditional IPAT model, the STIRPAT model, is used in our research (Wang et al., 2018), in which we select promising variables to examine the impact of economic growth, urbanization, and technology factors on carbon emissions. The STRIPAT model is expressed as follows

$$I = aP^b A^c T^d e \quad (9)$$

where I represents the impact of carbon emissions or other pollutants on the environment, P represents the population, A represents the level of affluence of a region, T represents the development level of science and technology, and e is the error term. Simultaneously taking the logarithms of both sides of Eq. (8) gives

$$\ln I = a + b \ln P + c \ln A + d \ln T + e \quad (10)$$

The STIRPAT model is employed because the coefficients a b, c, and d can be estimated as parameters and the variables in the model can be decomposed (Liu et al., 2015). Here, the term on the left side of Eq. (9) represents the per capita CO_2 emissions $(PCCO_2)$ of cities. The factors on the right side are explained as follows. First, economic growth is usually expressed as the per capita GDP, the natural logarithm (PGDP) and the squared value of the natural logarithm (PGDPsq) of which are used to examine the traditional EKC hypothesis and test whether there is an inverted U-shaped curve between the per capita CO_2 emissions and the economic growth of each city.

The second variable is the population urbanization rate (URB), which is equal to the ratio of the permanent population of cities and towns to the total permanent population in cities expressed as a fraction. According to previous studies, the total population size is often used as P (Wang et al., 2017). However, the dependent variable in this paper is the per capita carbon dioxide emissions; thus, we consider it appropriate to adopt the population urbanization rate to represent P.

Since the combustion of fossil energy from secondary industries (especially heavy industries) is an important component of anthropogenic carbon emissions, the third variable is the proportion of secondary industries (SIP). This variable is used to measure the impact of the industrial structure on the regional carbon emissions. Centralized heating, which exists only to the north of the Yangtze River in China, inevitably leads to the accelerated combustion of fossil fuels, such as coal, in most northern regions of China.

To explore the impact of this factor on carbon emissions, the average temperature in January (ATJ) is chosen as the fourth variable. Because of the lack of data at the city level, the expenditure ratio of science and technology (EST) expressed as a fraction is used to represent the technology level, with higher values representing greater investments in R&D in a given city. In addition, the investment in fixed assets (FAI) is used to analyze the impact of investment on carbon emissions. Given the same traffic volume, a denser road network indicates better accessibility in a city and, thus, a higher efficiency of vehicle exhaust emissions; therefore, the density of the road network (DRN) is considered a vital influencing factor.

The final variable is the utilization rate of foreign capital (UFC), which equals the ratio of the actual utilization of foreign capital to the gross domestic product expressed as a fraction, which represents the impact of the level of openness on urban carbon emissions.

Spatial data usually have the distinct feature of spatial

dependence, which means that adjacent regions have similar attributes and interact in many ways (Lesage, 2014). Previous studies have shown that spatial dependence is important for understanding the relationship between environmental pollutants and income (Rupasingha et al., 2010). The neglect of spatial dependence in examining the EKC may lead to errors in the estimation results (Maddison, 2006). To avoid this condition, spatial dependence is often measured by the spatial lag model (SLM) and spatial error model (SEM). SLM considers that the dependent variables of the neighboring units have an effect on the dependent variables, while SEM assumes that the spatial dependence in the error terms is more significant.

The formula for SLM is

$$Y = \alpha + \rho WY + \beta X + \varepsilon \tag{11}$$

while that for SEM is

$$Y = \alpha + \beta X + \varepsilon \tag{12}$$

$$\varepsilon = \lambda W\varepsilon + \mu \tag{13}$$

where $Y$is an n by 1 vector, which presents the dependent variable; $X$is an n by k matrix, which is composed of explanatory variables; W is the spatial weight matrix; α and λ denote scalar parameters, and β is a k by 1 vector, which is the regression coefficient.

Further model testing is necessary to determine which spatial econometric model to use for the regression. Ordinary least squares (OLS) is used before applying SLM and SEM. Generally, the Lagrange multiplier (LM-lag, LM-error) and the robust versions are used to determine the significance of the OLS results. The basic evaluation criteria are that if the LM-lag and LM-error are not significant, the OLS model is supported, and the spatial econometric model is rejected. Otherwise, if either the LM-lag or the LM-error is significant, the corresponding spatial econometric model is selected. If both are significant, then the significance of the robust LM-error and robust LM-lag is determined. If the robust LM-error is more significant, the SEM model is more appropriate. Otherwise, the SLM model is more appropriate (Anselin et al., 1996). In the present study, the dependent variable is the per capita CO_2 emissions of each city in China, while the explanatory variables are the PGDP, PGDPsq, URB, SIP, ATJ, EST, FAI, DRN, and UFC.

4. Results and discussion

4.1. Fitting accuracy using statistical data of CO_2 emissions at the provincial level

Using the energy consumption statistics and the estimation method described in 2.3.1, the carbon emissions are obtained for each province. Table 1 shows the CO_2 emissions data, population, GDP, and carbon intensity data of 27 provinces and the 4 municipalities directly under the central government (i.e., Beijing, Shanghai, Tianjin, and Chongqing). Shandong, Hebei, Shanxi, Jiangsu, and Inner Mongolia are the five highest total carbon emitters. Shandong and Jiangsu Provinces are also ranked at the top in terms of GDP and population. Pearson's correlation coefficient analysis shows that the coefficient relating the total carbon dioxide emissions and population is 0.658 ($P < 0.01$), while the coefficient relating the total carbon dioxide emissions and GDP is 0.652 ($P < 0.01$). The above 5 provinces are mostly located in northern China, which is consistent with previously reported findings (Wang and Ye, 2017). Of the southern provinces, Jiangsu Province has the highest total carbon emissions and ranks fourth in China, followed by Guangdong Province, ranking tenth, with Hainan having the least carbon emissions. This difference is mainly caused by the greater consumption of fossil energy in northern provinces to improve their industrial level, while relatively less fossil energy is consumed in southern provinces.

In terms of per capita CO_2 emissions, the provinces in northern China still rank the highest, with Inner Mongolia and Ningxia Province having the highest levels, producing emissions exceeding 30 tons, followed by Shanxi and Xinjiang Provinces, which have relatively high levels exceeding 20 tons. This phenomenon can be attributed to the higher total carbon emissions of these provinces relative to their smaller total populations. For example, Inner Mongolia, with a population of 24.7 million, is 23rd in the national ranking, but its total CO_2 emissions rank 5th. Similar situations are reflected in such provinces as Ningxia and Xinjiang. In addition, the intensity of carbon emissions can reflect whether a region's economic development model is low-carbon sustainable or extensive. Table 1 shows that economically developed areas usually have low carbon intensities, and emissions are generally lower in the southern provinces. For instance, Beijing, Guangdong, and Shanghai rank higher, while the provinces and municipalities in the south represent 8 of the top 10 provinces in terms of low carbon intensity.

Furthermore, the CO_2 emissions of each province are estimated using corrected NTL imaging, which is a combination of the NPP-VIIRS NTL values and population grid data. To test the accuracy of the new method, it is necessary to compare the total emissions from these two sources. In particular, the R^2 of the regression analysis and the mean relative error (MRE) are utilized.

Fig. 1 shows that the simulated and real carbon emission values are very close. The positive linear relationship between the CO_2 emissions estimated from the corrected NTL data and the calculated energy consumption data in each province of China is significant. As shown in Fig. 1(a), the R^2 value of the estimated emissions from the 2015 corrected NTL data is 0.8516, which indicates that the correlation between the simulated and statistical results is very strong. According to a comparison with the goodness of fit (R^2) observed in Ou et al.'s investigation of the U.S. states, there is little difference between our fitness and their results in simulating emissions using NTL-population datasets.

In addition to the high correlation, the MRE of the estimated result is 39.63%, exceeding that of Ou's result, which shows that the estimated values obtained from the corrected NTL data better fit the statistics at the provincial level (Ou et al., 2015). Furthermore, to measure the validity of this method, the carbon emissions from various provinces in China are estimated for 2016. Notably, the 2015 population grid is used as a substitute because no population grid exists for 2016 and the energy consumption data and NTL data for 2016 are available.

As shown in Fig. 1(b), the R^2 value of the emissions estimated using the corrected NTL data is 0.7498, which is slightly lower than the 2015 value, and the MRE is 46.83%. Overall, the goodness of fit is higher, supporting the advantages of this method for modeling China's CO_2 emissions.

Previous studies typically fitted the carbon emissions and the radiation values of NTL data directly and used the regression relationship between them to estimate the emissions value (Ma and Xiao, 2017; Meng et al., 2014; Wang and Li, 2016; Wang and Ye, 2017). In the present study, similar methods are employed to explore whether the method of using corrected NTL data is superior to the previous method, according to the goodness of fit of the carbon emissions estimation. As shown in the scatter plots in Fig. 2, the R^2 results of the radiance values obtained using the 2015 and 2016 statistics are 0.3247 and 0.4014, respectively, indicating that the fit between the original NPP data and CO_2 emissions statistics is relatively poor.

In addition, to reduce the heteroscedasticity of the NTL data and

Table 1
2015 provincial CO_2 emissions.

Province	CO_2 (10^4 t)	Population (10^4 person)	GDP (CNY 10^8)	CO_2 (t/person)	CO_2 (t/CNY10^4)
Beijing	14523.22	1961.20	23014.59	7.4052	0.6310
Tianjin	20924.04	1293.82	16538.19	16.1723	1.2652
Hebei	91786.57	7185.42	29806.11	12.7740	3.0795
Shanxi	86457.61	3571.21	12766.49	24.2096	6.7722
Inner Mongolia	83493.15	2470.63	17831.51	33.7942	4.6823
Liaoning	66009.16	4374.63	28669.02	15.0890	2.3024
Jilin	26281.63	2746.22	14063.13	9.5701	1.8688
Heilongjiang	37576.19	3831.22	15083.67	9.8078	2.4911
Shanghai	30571.17	2301.39	25123.45	13.2837	1.2168
Jiangsu	84563.65	7865.99	70116.38	10.7505	1.2060
Zhejiang	46457.65	5442.00	42886.49	8.5368	1.0832
Anhui	43245.36	5950.10	22005.63	7.2680	1.9652
Fujian	28355.78	3552.00	25979.82	7.9830	1.0914
Jiangxi	24189.68	4456.74	16723.78	5.4276	1.4464
Shandong	124254.10	9579.31	63002.33	12.9711	1.9722
Henan	69208.57	9402.36	37002.16	7.3607	1.8704
Hubei	40806.65	5723.77	29550.19	7.1293	1.3809
Hunan	35769.51	6568.37	28902.21	5.4457	1.2376
Guangdong	65985.17	10430.03	72812.55	6.3265	0.9062
Guangxi	21981.44	4602.66	16803.12	4.7758	1.3082
Hainan	5578.843	867.15	3702.76	6.4335	1.5067
Chongqing	19461.03	2884.00	15717.27	6.7479	1.2382
Sichuan	43741.48	8041.82	30053.10	5.4393	1.4555
Guizhou	31816.84	3476.65	10502.56	9.1516	3.0294
Yunnan	24656.57	4596.60	13619.17	5.3641	1.8104
Xizang	N/A	300.21	1026.39	N/A	N/A
Shaanxi	47208.51	3732.74	18021.86	12.6471	2.6195
Gansu	19801.37	2557.53	6790.32	7.7424	2.9161
Qinghai	6032.39	562.67	2417.05	10.7210	2.4958
Ningxia	20997.03	630.14	2911.77	33.3212	7.2110
Xinjiang	47297.70	2181.33	9324.80	21.6829	5.0722

Note: Tibet is not included due to the lack of energy consumption data.

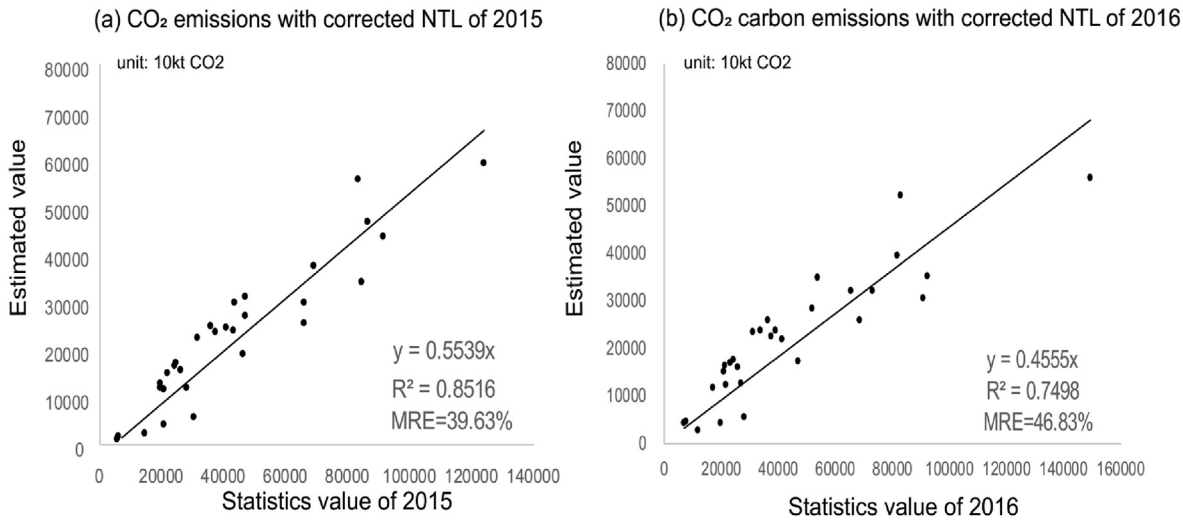

Fig. 1. Correlation between 2015 and 2016 provincial statistics values and estimated CO_2 emissions.

CO_2 emissions, log-log scatter plots are applied. As shown in Fig. 3, the R^2 of NTL with CO_2 emissions is 0.6248 for 2015 and 0.6778 for 2016. The goodness of fit of the double logarithmic function is significantly better than that of the original value scatter plots. These results indicate that the use of single NTL data alone does not outperform the combination of NTL and population data for estimating CO_2 emissions. Although Zhang et al. (2017) mention that NPP-VIIRS data used alone are inferior to DMSP-OLS data in estimating carbon emissions, our method and results effectively compensate for this deficiency. The simulation results based on the corrected NTL data are good, which demonstrates the feasibility of using NPP-VIIRS data for the rapid estimation of China's provincial carbon emissions.

4.2. Spatial distribution of CO_2 emissions at the city level

Fig. 4 shows the carbon emissions grid map derived from NTL data and population grid data according to the regression formula obtained at the provincial scale. The eastern coastal regions and the North China Plain tend to generate massive emissions. In contrast, vast western and middle regions have low emissions. The numerical differences between the grids are extremely large—the

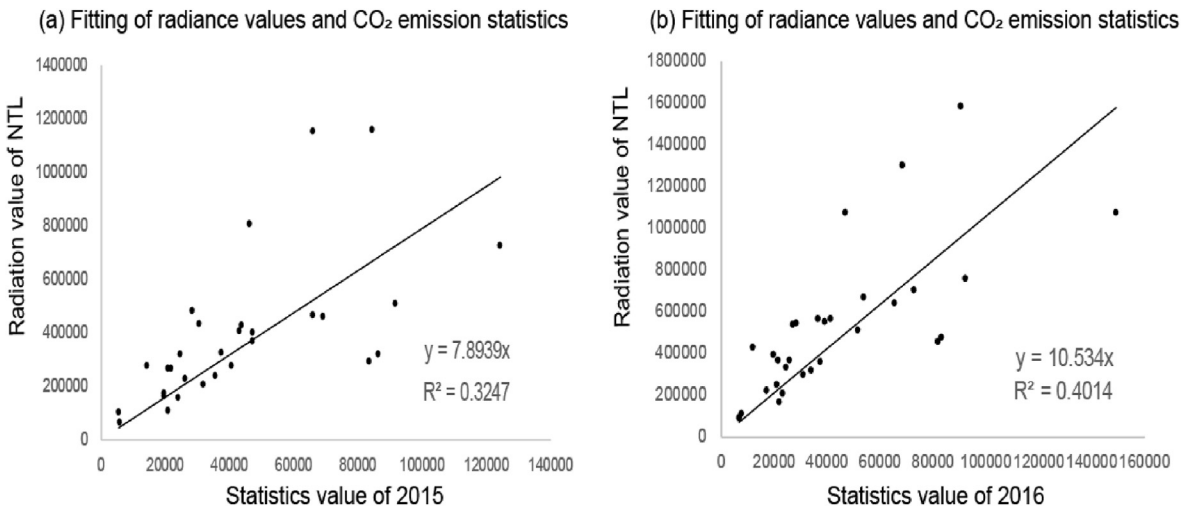

Fig. 2. Fitting relationship between the 2015 and 2016 radiance values of NTL and CO_2 statistics.

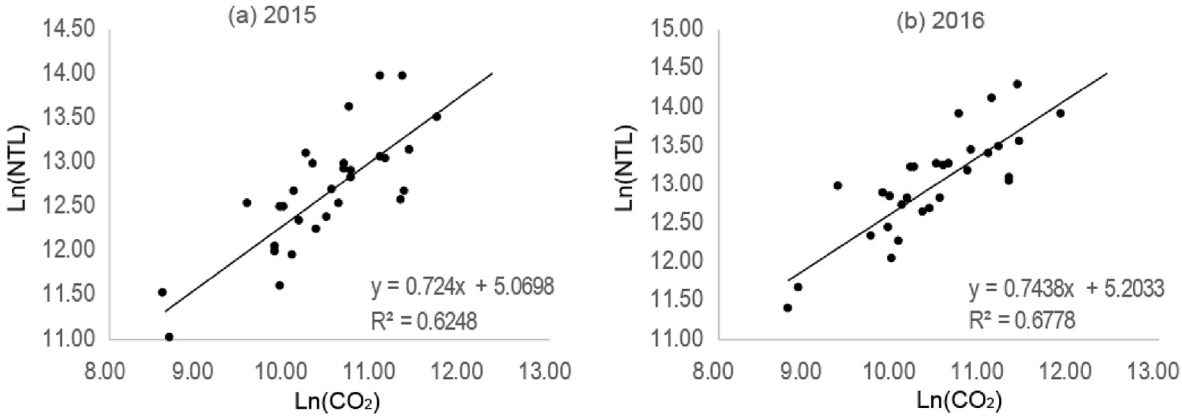

Fig. 3. 2015 and 2016 log-log function scatter plots of the radiance values of NTL and CO_2 statistics.

maximum carbon emission grid value is 15.19 million tons, while the minimum is close to zero tons.

Utilizing the zoning statistics tools of ArcGIS 10.2, the CO_2 emissions of each city are obtained (Fig. 5). The spatial distribution of China's city-level CO_2 emissions is uneven, presenting significant spatial variations. The CO_2 emissions of cities in the western, eastern, central, and northeast regions account for 34.63%, 30.40%, 24.90%, and 10.07% of the total emissions, respectively. Cities located in Beijing-Tianjin-Hebei, the Yangtze River Delta, and Inner Mongolia, such as Chifeng, Shanghai, Tongliao, Tianjin, and Baoding, have high CO_2 emissions. Moreover, cities with high emissions include, first, developed cities with great economic scales and large populations, such as Chongqing, Shanghai, Tianjin, Qingdao, and Suzhou, and second, such resource-constrained cities as Chifeng, Tongliao, Ordos, Ulanqab, Yuncheng, and Lvliang, where the dominant source of CO_2 emissions is industrial energy. Cities dominated by steel industrial production, such as Tangshan, Handan, Baoding, and Shijiazhuang, also contribute high emissions, generally due to their low efficiency and excessive use of fossil fuels.

Concerning the spatial distribution of CO_2, the shifting of CO_2 from affluent areas (such as Beijing and Shanghai) to poor areas (such as Hebei and Inner Mongolia) is also important. For example, through outsourcing and other means, goods such as cement and steel produced in Inner Mongolia are transported to richer regions. To regulate the industrial structure and reduce the pressure from population and environmental pollution in Beijing, the Shougang Group was transferred to Tangshan City, Hebei Province, in 2008.

In contrast, cities in southern China, such as Sanya, Fangchenggang, Yingtan, Danzhou, and Ezhou, have relatively low emissions levels. China's fossil energy resources, such as coal mines, oil, and natural gas, are less distributed in the southern regions (Shen et al., 2012). High-energy-consuming industries, such as the iron and steel industries dominated by high energy consumption, are also mainly distributed in the north. Compared with northern cities, which mainly focus on the energy industry, the industrial level of these southern cities is relatively poor, and tourism is often regarded as the main industry. This condition also contributes to their lower carbon emissions and lower environmental pressure. In addition, cities in Qinghai and Gansu Provinces have low emissions. The cities with the lowest emissions are located in the Tibetan autonomous prefectures and Gansu Province, which are economically lagging and lack energy resources.

In terms of per capita CO_2 emissions (Fig. 6(a)), there is distinct north-south differentiation. China's northern cities have much greater emissions than do the southern cities. The per capita carbon emissions of most southern cities are lower than the nationwide average of 12.96 tons—only the emissions of 17 of the 188 cities in the southern regions are higher. However, of the 110 cities in the northern regions, 40 produce above the average value. Unlike the situation revealed in Fig. 5, the per capita CO_2 emissions in Beijing-

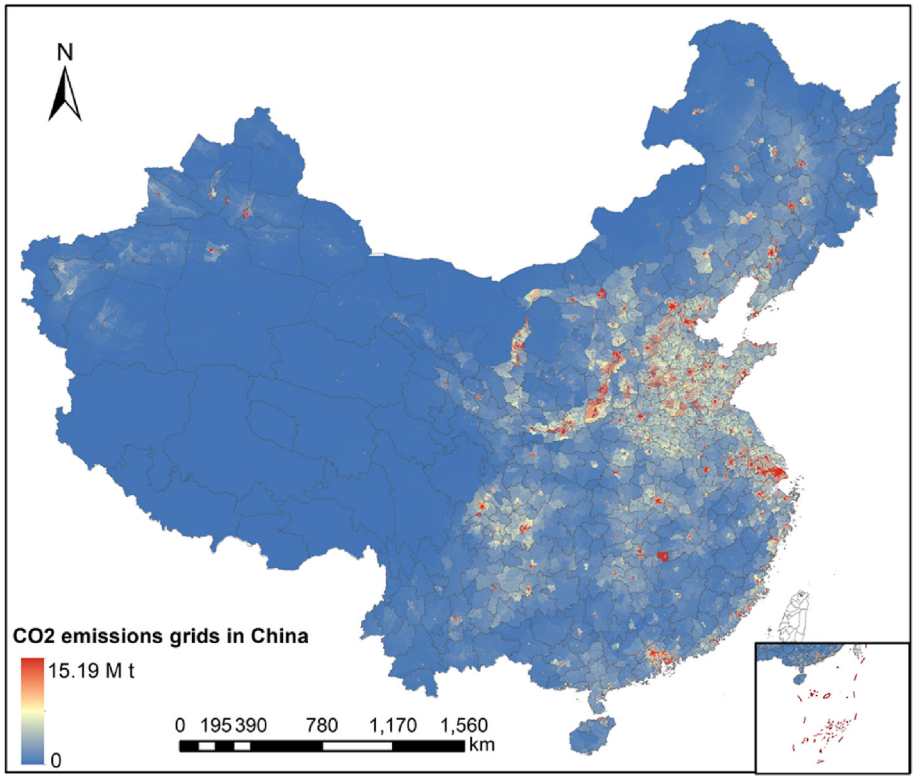

Fig. 4. CO_2 emissions grid map of China in 2015 (Base on map sources: GS(2019)1699).

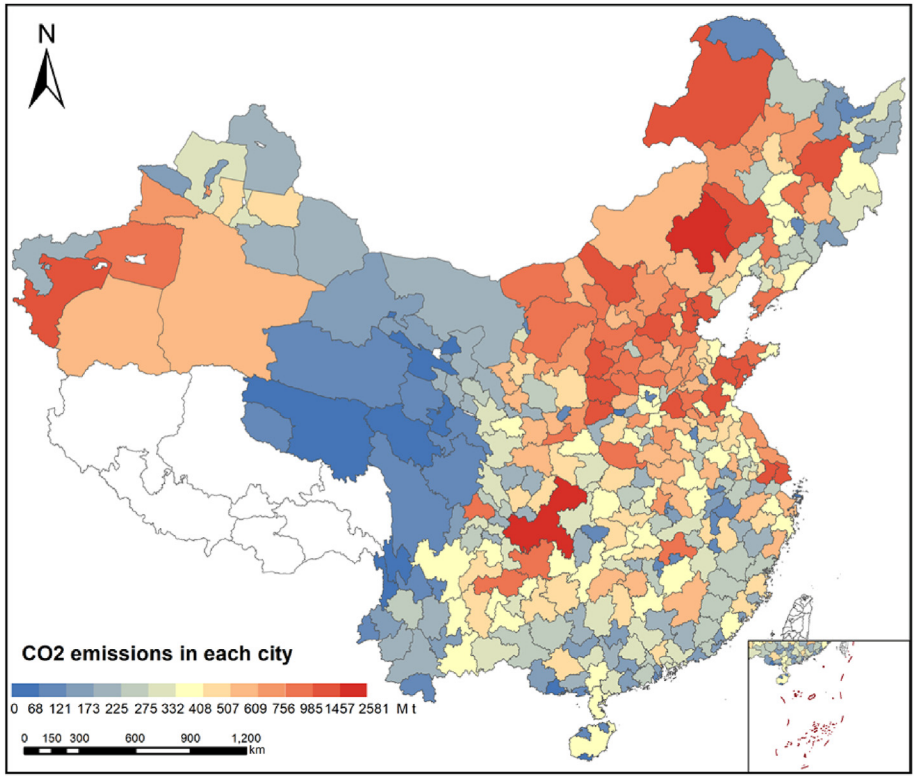

Fig. 5. CO_2 emissions in each city in 2015.

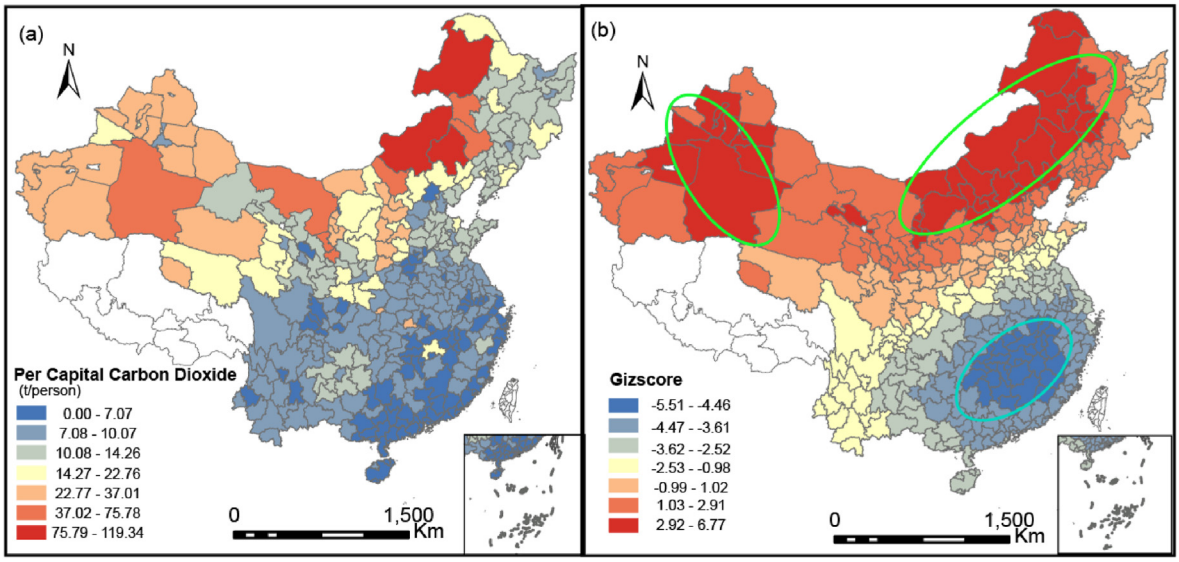

Fig. 6. Spatial distribution and cluster patterns of city-level per capita CO_2 emissions.

Tianjin-Hebei and the Yangtze River Delta are not high. Many cities in China's western region, such as those in Inner Mongolia and Xinjiang, have high per capita carbon emissions, and this is mainly related to the extensive mode of economic development, smaller urban population, and unique coal-dominated energy structure.

The global Moran's I index reflects the spatial correlation of CO_2 emissions at the national scale (Lanorte et al., 2013), while the Getis-Ord Gi* statistic is mainly used to observe the local similarities and differences between adjacent cities (Zhang et al., 2018).The Getis-Ord Gi* statistic is built on statistical inference experiments. For GIS spatial analysis, this statistic shows whether there is a statistically significant spatial clustering (hot spot) or dispersion (cold spot) phenomenon created by random processes within the space of a feature. The basic principle is to resample the data according to a certain neighborhood and determine whether the randomness of the spatial distribution is tenable according to the deviation degree of the local data mean relative to the overall mean value. The assumption is that the elements are randomly and independently distributed within the spatial distribution, so the results calculated according to the spatial weighting are bound to show a normal distribution. Gi* is actually GiZscore. The more GiZscore tends toward both ends, the lesser is the probability that the distance hypothesis is established. When the GiZscore exceeds the significance, the hypothesis is overturned. Through the calculation of the GiZscore, we can determine how far the mean value of the study area deviates from the overall mean value. When it exceeds the confidence level (for example, 90%), we will overturn the hypothesis, which shows that there is statistically significant clustering or dispersion in the spatial distribution of the feature characteristics, and the hypothesis of random distribution is not tenable (Getis and Ord, 1992).

In the present study, the global Moran's I index (0.131, p-value<0.001, GiZscore = 14.09) indicates a significant spatial correlation among the cities' per capita CO_2 emissions. To understand the characteristics of emissions agglomeration from the local perspective, the GiZScore for each city is visualized (Fig. 6(b)). The most underdeveloped cities in the western and northern regions have high scores in the range of 1.03−2.91 ($p < 0.05$) and 2.92−6.77 ($p < 0.001$). The GiZScores of cities located south of the Yangtze River are relatively low, within the ranges of −4.47 to −3.61 ($p < 0.05$) and −5.51 to −4.46 ($p < 0.001$). There is obvious spatial clustering of the city CO_2 emissions, with two evident hot-spot regions in the border area of Inner Mongolia-Jilin-Hebei-Shanxi-Ningxia and the central regions of Xinjiang and one cold-spot region located in the border area of Jiangxi-Hunan-Fujian-Anhui.

Table 2
OLS regression result.

Variable	Coefficient	*t*-statistic	*p*-value
Constant	−14.688*	−1.884	0.060
PGDP	2.550*	1.801	0.072
PGDPsq	−0.113*	−1.737	0.083
URB	−0.235	−1.576	0.115
SIP	0.141	1.435	0.152
ATG	−0.032***	−10.904	0.000
EST	−0.092**	−2.505	0.012
FAI	0.056*	0.032	0.088
DRN	−0.433***	−4.693	0.000
UFC	−0.019	−1.500	0.134
	R^2	0.518	
	Adjusted R-squared	0.503	
	Log likelihood	−104.668	

Note: *, **, and *** denote significance at the 0.10, 0.05, and 0.01 levels, respectively.

4.3. Evidence of the EKC from spatial econometric modeling

As mentioned in Section 2.3.3, OLS regression is applied before the selection of SLM and SEM. According to the regression results (Table 2), the R^2 is 0.518, and the adjusted R^2 is 0.503. The variables PGDP, PGDPsq, FAI, ATJ, and DRN pass the significance test at the 0.10 level, while EST passes at the 0.005 level. These good results of the OLS model make it useful for testing the EKC hypothesis.

In Table 3, the LM diagnostics for the spatial dependence of the linear models suggest that LM-lag ($p < 0.001$) and LM-error ($p < 0.001$), as well as their robust versions ($p = 0.033$ and $p < 0.001$), are significant. This finding indicates that both the SLM and SEM are eligible to be applied to interpret the coefficient estimates (Brunsdon et al., 2010). However, the AIC of the SEM is higher than that of the SLM, and the SLM and SEM goodness of fit values (R^2) are 0.67 and 0.60, respectively. Considering that the SLM accounts for the impact of neighboring cities on a given city's CO_2 emissions, the positive Moran's I index and local Getis-Ord Gi* Z-

Table 3
SLM and SEM regression parameters.

	SLM			SEM		
	Coefficient	*t*-statistic	*p*-value	Coefficient	*t*-statistic	*p*-value
Constant	−15.794**	−2.251	0.024	−9.357	−1.482	0.138
PGDP	1.755**	2.161	0.030	1.758	1.547	0.121
PGDPsq	−0.123**	−2.099	0.035	−0.083	−1.595	0.110
URB	−0.217	−1.611	0.106	−0.231*	−1.861	0.062
SIP	0.091**	1.021	0.033	0.289***	3.367	0.000
ATG	−0.019***	−5.881	0.000	−0.011**	−2.301	0.021
EST	−0.070**	−2.115	0.034	−0.071**	−2.091	0.036
FAI	0.032	1.092	0.274	0.042	1.511	0.130
DRN	−0.352***	−4.145	0.000	−0.521***	−5.477	0.000
UFC	−0.018	−1.600	0.109	−0.017	−1.534	0.124
⟩	0.375***	6.707	0.000			
				−9.357	−1.482	0.138
Log likelihood		−83.692			−98.020	
AIC		195.385			207.041	

Lagrangian multiplier (LM) diagnostics for the spatial dependence of the linear models

	Statistic	**p-Value**
LM error	67.994***	0.000
LM lag	45.154***	0.000
Robust LM error	24.110***	0.000
Robust LM lag	7.270**	0.033

score in Fig. 4 indicate the existence of spatial dependence. We therefore focus on the regression results of the SLM model.

As expected, the SLM indicates that the per capita GDP and its squared term, which represents the level of affluence of cities, are significantly correlated with the per capita carbon emissions at the 0.05 level. The coefficient of PGDP is positive (1.755), indicating that a 1% increase in wealth per capita would lead to an average 1.755% rise in per capita CO_2 emissions. The PGDPsq coefficient is negative (−0.123), which implies that there is an inverted U-shaped relationship between the wealth level and the intensity of CO_2 emissions. In other words, per capita carbon emissions increase with the increase of the per capita GDP. When the per capita GDP reaches a certain level, the intensity of carbon emissions tends to decrease with the increase of the per capita GDP. In addition, based on the PGDP coefficient and its squared term, the per capita GDP corresponding to the inflection point of CNY 73,071 per capita carbon emissions is obtained. This finding also confirms that China's 2015 CO_2 emissions level is still on the left side of the Kuznets curve, i.e., the CO_2 emissions level is not decoupled from economic growth.

In Table 4, only 17.53% of all cities exceed this inflection point. Most cities in the country are still a considerable distance from the turning point of the decoupling of economic development from carbon emissions. The east, central, west, and northeast areas account for 62.74%, 11.76%, 15.68%, and 9.82%, respectively, of the cities crossing the inflection point. It can be seen that the economic development gap between regions has a great impact on the decoupling state, and economically developed regions can take the lead in decoupling. However, as far as the four major regions are concerned, 31 cities in the eastern region reach this inflection point, accounting for 36.36% of all cities in the region. Correspondingly, the proportions of central, western, and northeastern regions reached 7.5%, 9%, and 14.29%, respectively. Therefore, even within the regions, eastern-region cities are still the first, indicating that this region is absolutely dominant in achieving the decoupling of carbon emissions, with the northeastern region also having a relative advantage. The absolute and relative rankings of the central and western regions are not dominant in the decoupling status of carbon emissions.

However, although the inflection point is calculated, it does not mean that when the inflection point is reached, the national level of carbon emissions will begin to decline with economic growth (Riti et al., 2017). Moreover, the EKC turning point calculated in the present study is inconsistent with the results of other studies in China. In fact, there is no consensus on the level of per capita wealth at peak CO_2 emissions, which can be attributed to the susceptibility of this inflection point to data sources, research time limits, and the variables involved. Thus, the result may still indicate the existence of the CO_2 emission Kuznets curve and that it has not yet arrived at its inflection point.

The SIP positively affects CO_2 emissions, with a coefficient value of 0.091. China's industrial structure is the main reason for the increase in carbon emissions (Zhang, 2012). In 34% of the cities considered here, the 2015 secondary industry output value as a proportion of the total output reached 50% or more. Additionally, the increase in the secondary output value of these cities is mostly from high-intensity energy consumption and emissions. However, the efficiency of production output and energy conversion is relatively low, which implies that many cities in China, especially those dependent on heavy and mineral industries, need to consider transforming their urban development path. In contrast, the per capita carbon emissions are relatively low in economically developed cities due to the implementation of environmental

Table 4
Number and proportion of cities reaching inflection points in different regions.

	East	Central	West	Northeast	Sum
Total cities	88	80	88	35	291
Cities reaching inflection points	32	6	8	5	51(17.53%)
Total Proportion (%)	62.74	11.76	15.68	9.82	100
Region proportion (%)	36.36	7.50	9.00	14.29	/

regulations, the reduction of excess capacity, and industrial transformation and upgrading strategies. The impact of FAI is not significant ($p = 0.274$), contrary to Fu et al.'s (2014) finding that many investment-driven cities have high carbon emissions.

The carbon emissions and such remaining variables as ATJ, EST, and DRN are negatively correlated. ATJ, for example, has a significant ($p < 0.001$) negative effect on per capita CO_2 emissions, with a 1% increase of the former being associated with a 0.019% decrease of the latter. In China's northern cities, the lower the ATJ and the more days low temperatures persist, the greater is the pressure on the national heating system, which means that more coal is consumed to provide centralized heating for urban residents. Additionally, coal is used for heating or cooking in most rural regions, despite being a direct energy source with an extremely low efficiency of only 30% (Wang and Mendelsohn, 2003). The temperature therefore has an indirect impact on CO_2 emissions. Given the consequences of using coal as an energy source, aging heating equipment needs to be replaced, and such new energy sources as wind and geothermal energy are also being considered as substitutes. Additionally, the influences of different energy sources on regional soil and water resources are important (Hong et al., 2013; Yang et al., 2013). The southern region has fewer emissions because of its higher winter temperatures and the shorter duration of colder weather that does not require heating equipment.

The EST reflects the relationship between emissions and the level of science and technology, as measured by the proportion of science and technology expenditure. Generally, technological progress tends to increase the energy efficiency and result in lower volumes of CO_2 being emitted with the same level of production (Rosa, 2003). As expected, our model indicates that the EST exerts a significant ($p = 0.034$) negative influence on per capita emissions, as suggested in previous studies (Liu et al., 2010; Wang and Huang, 2019), and this implies that improving the technological level can reduce CO_2 emissions. However, some hold an opposing view (Hang and Jiang, 2011), insisting that the social and economic returns from technological advances stimulate additional production and lead to the use of higher amounts of fossil energy, despite the increased efficiency. As Wang and Huang (2019) demonstrated, technological progress is the main source of emissions reduction in regions with low carbon emissions, with the contribution of technological progress to emissions reduction being nonsignificant in areas with high carbon emission intensities.

A higher-density road network contributes to reduced CO_2 emissions, and the coefficient term is significant at the 1% level, which signifies that a 1% increase in the DRN results in an average 0.352% decrease in per capita emissions. Improvements in such urban infrastructure as roads can notably improve the efficiency of motor vehicles, especially in large cities, thus alleviating the pressure of carbon emissions from transportation energy, which is a finding in support of Wang et al. (2018).

The coefficient of UFC is not significant, indicating that foreign capital has no influence on CO_2 emissions. The extent to which FDI affects the environment is a controversial issue (Pazienza, 2014), as there is a counterargument that FDI causes more CO_2 emissions in China, which is consistent with the pollution haven hypothesis (Jun et al., 2018). Regional differences in human capital contributions and environmental regulations also determine whether FDI has a positive or negative impact on carbon emissions (Li et al., 2019). The URB coefficient is also nonsignificant ($p = 0.106$), which contradicts Xu et al. (2018) finding that urbanization has a negative influence on emissions or that urbanization contributes to the EKC in terms of carbon emissions (Wang and Zhou, 2012; Ahmed et al., 2019).

Finally, $\rangle$ represents the coefficient of the SLM model. At the 0.001 significance level, there is a 0.35% increase in a city's CO_2 emissions when the CO_2 emissions of its neighbors increase by 1%.

4.4. Advantages and limitations of this study

In this study, the corrected NTL combined with the original NPP-VIIRS NTL and population data are successfully employed to detect the spatial distribution of CO_2 emissions for each city in China. The study tests and verifies that the CO_2 estimation model proposed by Ghosh et al. (2010) is also applicable to Chinese provinces and cities. These findings reveal a highly linear relationship between the actual statistics and estimated emissions of each province in China. While Ou et al. (2015) examine this model using the actual 2012 statistics and estimated emissions for each U.S. state, the present study focuses on the applicability of the new method for China in 2015. Moreover, the EKC hypothesis is re-examined and validated, and emissions at the city level are explained for the implementation of precise carbon-reducing policies, which is the greatest benefit of the study. This study is a meaningful attempt to apply the NPP-VIIRS nighttime light data to the estimation of carbon dioxide emissions in China. The DMSP-OLS nighttime light data used by previous scholars are no longer produced and updated. With the continued release and updating of NPP-VIIRS data, in the future, this method can be used to reduce the carbon dioxide emissions space to a smaller geographic scale and a longer time scale. Research on characteristics and influencing factors can provide a clear understanding of China's carbon dioxide emissions and guide recommendations for relevant decision-making departments to formulate emissions reduction policies.

In utilizing corrected NTL data to estimate CO_2 emissions at the city level, this study is limited in that only a few cities recorded their energy consumption data in 2015, while the statistical yearbook data are also not necessarily reliable, which makes it difficult to test the estimates on the city scale. Moreover, although based at the city level, the step testing of the EKC hypothesis analyzes the macro factors that affect China's carbon emissions. However, due to space constraints, only the carbon emissions strategies for certain typical high-emitting cities are developed, with no specific emissions reduction strategies offered for each city individually. Furthermore, the EKC turning point approach used may be controversial, mainly due to the susceptibility of this inflection point to the data source, limited research time, and variables selected. However, the results can still be used as evidence in cooperation with other variables to show that China's CO_2 emissions are far from reaching an inflection point. Therefore, the relevance of this approach is not in passively waiting for the arrival of the inflection point but in the need to contain or reduce CO_2 emissions and developing corresponding environmental policies based on the analysis of the influencing factors. A final point is that because of data availability, cross-sectional data are used for spatial econometric regression for only one year, making it worthwhile for future research to consider longer periods.

5. Conclusions

This study uses corrected nighttime light data, which combine the original NPP-VIIRS data and population data to estimate the amount of 2015 CO_2 emissions produced by various provinces in China. The CO_2 emissions statistics obtained from the energy consumption data are then employed to verify the estimated values. The process and results demonstrate that this estimation method is feasible for studying China's CO_2 emissions. The linear relationship obtained at the provincial scale by applying the corrected NPP-VIIRS data of cities is then used to explore the CO_2 spatial distributions at the city scale in China to produce interesting conclusions. Finally, the spatial economic model is used to verify the EKC of CO_2

emissions and explore the potential social and economic factors that may have contributed to CO_2 emissions. The main conclusions are summarized as follows.

(1) The empirical findings first show that at the provincial level, China's total 2015 CO_2 emissions were high in such northern provinces as Shandong, Hebei, Shanxi, and Inner Mongolia. Of the southern provinces, Jiangsu and Guangdong rank the highest in terms of carbon intensity, with such developed regions as Beijing, Guangdong, Shanghai, and certain southern provinces having relatively low carbon intensity levels. The results show that the northern region in China will experience greater pressure to reduce emissions in the future.

(2) The top-down method of CO_2 allocation using corrected NTL data by combining population data and the original NPP data is proposed as a more feasible and credible approach compared to previous methods. This method has strong practicality and can be used to explore the characteristics of carbon dioxide distributions in the long-term future. The spatial distribution characteristics revealed in this way indicate that China's emissions are uneven overall. Western regions in China emitted the most CO_2, and industrial and mining cities or developed cities had higher total carbon emissions values. This finding suggests new requirements for cities dominated by industry and mining. These cities should pay attention to adjusting the industrial structure and gradually changing the development model away from a single-pillar industry that depends on energy resources. Per capita CO_2 emissions at the city level presented distinctly different north-south characteristics. The carbon emissions in many southern cities were below the national average. Such developed cities as Beijing, Tianjin, Shanghai, and Guangzhou had low-level emissions, and although the per capita carbon dioxide level is low, the government should consider the subsequent negative impact on the resources and the environment caused by continuous population influx to affluent cities, such as the increase in fossil fuel consumption caused by population increases. Most cities in Xinjiang and Inner Mongolia had high emission levels, and the per capita CO_2 emissions had clear spatial agglomeration characteristics. Meanwhile, cities in Mongolia-Jilin-Hebei-Shanxi-Ningxia and Xinjiang constituted two hot-spot regions, while cities in Jiangxi-Hunan-Fujian-Anhui constituted cold-spot regions.

(3) An EKC between CO2 emissions and per capita wealth level is shown to exist, with the results suggesting that a 1% increase in per capita wealth led to an average 1.755% increase in per capita CO_2 emissions. The EKC turning point hovered around CNY 73,071, and 16.7% of cities having crossed the turning point, with cities from eastern regions accounting for the largest proportion. The SIP had a positive effect on the level of CO_2 emissions, while the ATJ, EST, and DRN had a negative effect, with URB, FAI, and UFC having no significant impact. This finding shows that economic growth and carbon dioxide emissions have not been completely decoupled. For a long time to come, reducing carbon dioxide emissions will still be a focus that governments at all levels need to consider. Applying scientific and technological progress and increasing scientific and technological inputs to increase the efficiency of fossil energy consumption are areas facilitating the achievement of such reductions. The strong grasp of carbon emissions also shows that we must guide tertiary industry—mainly service industries—to account for the entire industry and eliminate certain inefficient and highly polluting secondary-industry enterprises.

Credit author statement

H.C. and X.Z. designed the research; H.C. and R.W. performed the research; X.Z. analyzed the data; H.C. drafted the manuscript, which was revised by X.Z. and T.C.; All authors have read and approved the final manuscript.

Declaration of competing interest

The authors declare that they have no known competing financial interests or personal relationships that could have appeared to influence the work reported in this paper.

Acknowledgements

This work was supported by the Strategic Priority Research Program of the Chinese Academy of Sciences, Pan-Third Pole Environment Study for a Green Silk Road (Pan-TPE) [grant number: XDA20040400]; the National Natural Science Foundation of China [grant numbers: 71834005, 71303203, 71673232]; the Research Grant Council of Hong Kong, China [grant number: CityU 11271716]; and the CityU Internal Funds [grant numbers: 9680195, 9610386].

References

Ahmed, Z., Wang, Z.H., Ali, S., 2019. Investigating the non-linear relationship between urbanization and CO_2 emissions: an empirical analysis. Air Qual. Atmos. Health 12 (8), 945–953. https://doi.org/10.1007/s11869-019-00711-x.

Ang, J.B., 2009. CO_2 emissions, research and technology transfer in China. Ecol. Econ. 68 (10), 2658–2665. https://doi.org/10.1016/j.ecolecon.2009.05.002.

Anselin, L., Bera, A.K., Florax, R., Yoon, M.J., 1996. Simple diagnostic tests for spatial dependence. Reg. Sci. Urban Econ. 26 (1), 77–104. https://doi.org/10.1016/0166-0462(95)02111-6.

Brown, M.A., Southworth, F., Sarzynski, A., 2009. The geography of metropolitan carbon footprints. Policy and Society 27 (4), 285–304. https://doi.org/10.1016/j.polsoc.2009.01.001.

Brunsdon, C., Fotheringham, A.S., Charlton, M.E., 2010. Geographically weighted regression: a method for exploring spatial nonstationarity. Geogr. Anal. 28 (4), 281–298. https://doi.org/10.1111/j.1538-4632.1996.tb00936.x.

Cai, B., Guo, H., Cao, L., Guan, D., Bai, H., 2018a. Local strategies for China's carbon mitigation: an investigation of Chinese city-level CO2 emissions. J. Clean. Prod. 178, 890–902. https://doi.org/10.1016/j.jclepro.2018.01.054.

Cai, B., Liang, S., Zhou, J., Wang, J., Cao, L., Qu, S., Xu, M., Yang, Z., 2018b. China high resolution emission database (CHRED) with point emission sources, gridded emission data, and supplementary socioeconomic data. Resour. Conserv. Recycl. 129, 232–239. https://doi.org/10.1016/j.resconrec.2017.10.036.

Chai, B., Li, P., Zhang, R., Zhao, P., 2016. Urban expansion extraction using landsat series data and DMSP/OLS nighttime light data: a case study of Tianjin area. Acta Sci. Nauralium Univ. Pekin. https://doi.org/10.13209/j.0479-8023.2015.138.

Chen, G., Shan, Y., Hu, Y., Tong, K., Wiedmann, T., Ramaswami, A., Guan, D., Shi, L., Wang, Y., 2019. Review on city-level carbon accounting. Environ. Sci. Technol. 53 (10), 5545–5558. https://doi.org/10.1021/acs.est.8b07071.

Cheng, Y., Wang, Z., Zhang, S., Ye, X., Jiang, H., 2013. Spatial econometric analysis of carbon emission intensity and its driving factors from energy consumption in China. Acta Geograph. Sin. 68 (4), 1418–1431 (in Chinese).

Cui, C., Shan, Y., Liu, J., Yu, X., Wang, H., Wang, Z., 2019. CO2 emissions and their spatial patterns of Xinjiang cities in China. Appl. Energy 252. https://doi.org/10.1016/j.apenergy.2019.113473.

Elvidge, C.D., Baugh, K.E., Sutton, P.C., Bhaduri, B., Tuttle, B.T., Ghosh, T., Ziskin, D., Erwin, E.H., 2011. Who's in the dark-satellite based estimates of electrification rates. Office of Scientific & Technical Information Technical Reports. https://doi.org/10.1002/9780470979563.ch15.

Elvidge, C.D., Keith, D.M., Tuttle, B.T., Baugh, K.E., 2010. Spectral identification of lighting type and character. Sensors 10 (4), 3961–3988. https://doi.org/10.3390/s100403961.

Fan, J.-L., Wang, Q., Yu, S., Hou, Y.-B., Wei, Y.-M., 2016. The evolution of CO_2 emissions in international trade for major economies: a perspective from the global supply chain. Mitig. Adapt. Strategies Glob. Change 22 (8), 1229–1248. https://doi.org/10.1007/s11027-016-9724-x.

Fu, F., Ma, L.W., Li, Z., Polenske, K.R., 2014. The implications of China's investment-driven economy on its energy consumption and carbon emissions. Energy

Convers. Manag. 85, 573–580. https://doi.org/10.1016/j.enconman.2014.05.046.
Getis, A., Ord, J.K., 1992. The analysis of spatial association by use of distance statistics. Geogr. Anal. 24 (3), 189–206. https://doi.org/10.1111/j.1538-4632.1992.tb00261.x.
Ghosh, T., Elvidge, C.D., Sutton, P.C., Baugh, K.E., Ziskin, D., Tuttle, B.T., 2010. Creating a global grid of distributed fossil fuel CO_2 emissions from nighttime satellite imagery. Energies 3 (12), 1895–1913. https://doi.org/10.3390/en3121895.
Griggs, D.J., Noguer, M., 2010. Climate change 2001: the scientific basis. Contribution of working Group I to the third assessment Report of the intergovernmental panel on climate change. Weather 57 (8), 267–269. https://doi.org/10.1256/004316502320517344.
Guan, D.B., Klasen, S., Hubacek, K., Feng, K.S., Liu, Z., He, K.B., Geng, Y., Zhang, Q., 2014. Determinants of stagnating carbon intensity in China. Nat. Clim. Change 4 (11), 1017–1023. https://doi.org/10.1038/nclimate2388.
Hang, G., Jiang, Y.S., 2011. The relationship between CO_2 emissions, economic scale, technology, income and population in China. Proc. Environ. Sci. 11 (1), 1183–1188. https://doi.org/10.1016/j.proenv.2011.12.178.
He, C., Huang, Z., Ye, X., 2014. Spatial heterogeneity of economic development and industrial pollution in urban China. Stoch. Environ. Res. Risk Assess. 28 (4), 767–781. https://doi.org/10.1007/s00477-013-0736-8.
Hong, Y., Flower, R.J., Thompson, J.R., 2013. Shale gas: pollution fears in China. Nature 499 (7457), 154. https://doi.org/10.1038/499154b.
Jiang, J.H., Zhang, J.Y., Zhang, Y.W., Zhang, C.L., Tian, G.M., 2016. Estimating nitrogen oxides emissions at city scale in China with a nightlight remote sensing model. Sci. Total Environ. 544, 1119–1127. https://doi.org/10.1016/j.scitotenv.2015.11.113.
Jiang, X.T., Wang, Q., Li, R.R., 2018. Investigating factors affecting carbon emission in China and the USA: a perspective of stratified heterogeneity. J. Clean. Prod. 199, 85–92. https://doi.org/10.1016/j.jclepro.2018.07.160.
Jing, Q., Bai, H., Luo, W., Cai, B., Xu, H., 2018. A top-bottom method for city-scale energy-related CO2 emissions estimation: a case study of 41 Chinese cities. J. Clean. Prod. 202, 444–455. https://doi.org/10.1016/j.jclepro.2018.08.179.
Jun, W., Zakaria, M., Shahzad, S.J.H., Mahmood, H., 2018. Effect of FDI on pollution in China: new insights based on wavelet approach. Sustainability 10 (11), 20. https://doi.org/10.3390/su10113859.
Kang, J., Zhao, T., Ren, X., Lin, T., 2012. Using decomposition analysis to evaluate the performance of China's 30 provinces in CO_2 emission reductions over 2005–2009, 64 (2), 999–1013. https://doi.org/10.1007/s11069-012-0212-7.
Kang, Y.-Q., Zhao, T., Yang, Y.-Y., 2016. Environmental Kuznets curve for CO_2 emissions in China: a spatial panel data approach. Ecol. Indicat. 63, 231–239. https://doi.org/10.1016/j.ecolind.2015.12.011.
Karl, T.R., Trenberth, K.E., 2003. Modern global climate change. Science 302 (5651), 1719–1723. https://doi.org/10.1126/science.1090228.
Lanorte, A., Danese, M., Lasaponara, R., Murgante, B., 2013. Multiscale mapping of burn area and severity using multisensor satellite data and spatial autocorrelation analysis. Int. J. Appl. Earth Obs. Geoinf. 20, 42–51. https://doi.org/10.1016/j.jag.2011.09.005.
Lesage, J.P., 2014. Spatial econometric panel data model specification: a Bayesian approach. Spatial Statistics 9, 122–145. https://doi.org/10.1016/j.spasta.2014.02.002.
Li, B., Liu, X., Li, Z., 2015. Using the STIRPAT model to explore the factors driving regional CO_2 emissions: a case of Tianjin, China. Nat. Hazards 76 (3), 1667–1685. https://doi.org/10.1007/s11069-014-1574-9.
Li, F., Xu, Z., Ma, H., 2018. Can China achieve its CO2 emissions peak by 2030? Ecol. Indicat. 84, 337–344. https://doi.org/10.1016/j.ecolind.2017.08.048.
Li, J., Huang, X., Yang, H., Chuai, X., Li, Y., Qu, J., Zhang, Z., 2016. Situation and determinants of household carbon emissions in Northwest China. Habitat Int. 51, 178–187. https://doi.org/10.1016/j.habitatint.2015.10.024.
Li, W., Zhao, T., Wang, Y.N., Zheng, X.D., Yang, J.X., 2019. How does foreign direct investment influence energy intensity convergence in China? Evidence from prefecture-level data. J. Clean. Prod. 219, 57–65. https://doi.org/10.1016/j.jclepro.2019.02.025.
Li, X., Xu, H., 2020. The energy-conservation and emission-reduction paths of industrial sectors: evidence from chinas 35 industrial sectors. Energy Econ. 86 https://doi.org/10.1016/j.eneco.2019.104628.
Li, X., Xu, H., Chen, X., Li, C., 2013. Potential of NPP-VIIRS nighttime light imagery for modeling the regional economy of China. Rem. Sens. 5 (6), 3057–3081. https://doi.org/10.3390/rs5063057.
Liu, Z., Guan, D., Moore, S., Lee, H., Su, J., Zhang, Q.J.N., 2015. Climate policy: steps to China's carbon peak. Nature 522 (7556), 279–281. https://doi.org/10.1038/522279a.
Liu, Z., He, C., Zhang, Q., Huang, Q., Yang, Y., 2012. Extracting the dynamics of urban expansion in China using DMSP-OLS nighttime light data from 1992 to 2008. Landsc. Urban Plann. 106 (1) https://doi.org/10.1016/j.landurbplan.2012.02.013, 0-72.
Liu, Z., Wang, A., Yu, W., Li, M., 2010. Research on regional carbon emissions in China. Acta Geosci. Sin. 31 (5), 727–732 (in Chinese).
Lu, J., Vecchi, G.A., Reichler, T., 2007. Expansion of the Hadley cell under global warming (vol 34, art no L06805, 2007). Geophys. Res. Lett. 34 (14) https://doi.org/10.1029/2007gl030931.
Lv, Q., Liu, H., Wang, J., Liu, H., Shang, Y., 2020. Multiscale analysis on spatiotemporal dynamics of energy consumption CO2 emissions in China: utilizing the integrated of DMSP-OLS and NPP-VIIRS nighttime light datasets. Sci. Total Environ. 703, 134394. https://doi.org/10.1016/j.scitotenv.2019.134394.
Ma, X., Wang, C., Dong, B., Gu, G., Chen, R., Li, Y., Zou, H., Zhang, W., Li, Q., 2019. Carbon emissions from energy consumption in China: its measurement and driving factors. Sci. Total Environ. 648, 1411–1420. https://doi.org/10.1016/j.scitotenv.2018.08.183.
Ma, Z., Xiao, H., 2017. Spatiotemporal simulation study of China's provincial carbon emissions based on satellite night lighting data. China Population, Resources and Environment 27 (9), 143–150 (in Chinese).
Maddison, D., 2006. Environmental Kuznets curves: a spatial econometric approach. J. Environ. Econ. Manag. 51 (2), 218–230. https://doi.org/10.1016/j.jeem.2005.07.002.
Meng, L., Graus, W., Worrell, E., Huang, B., 2014. Estimating CO_2 (carbon dioxide) emissions at urban scales by DMSP/OLS (Defense Meteorological Satellite Program's Operational Linescan System) nighttime light imagery: methodological challenges and a case study for China. Energy 71, 468–478. https://doi.org/10.1016/j.energy.2014.04.103.
Mu, H.L., Li, H.N., Zhang, M., Li, M., 2013. Analysis of China's carbon dioxide flow for 2008. Energy Pol. 54, 320–326. https://doi.org/10.1016/j.enpol.2012.11.043.
Nicholson-Cole, S.A., 2005. Representing climate change futures: a critique on the use of images for visual communication. Comput. Environ. Urban Syst. 29 (3), 255–273. https://doi.org/10.1016/j.compenvurbsys.2004.05.002.
Omri, A., Euchi, J., Hasaballah, A.H., Al-Tit, A., 2019. Determinants of environmental sustainability: evidence from Saudi arabia. Sci. Total Environ. 657, 1592–1601. https://doi.org/10.1016/j.scitotenv.2018.12.111.
Ou, J., Liu, X., Li, X., Li, M., Li, W., 2015. Evaluation of NPP-VIIRS nighttime light data for mapping global fossil fuel combustion CO_2 emissions: a comparison with DMSP-OLS nighttime light data. PloS One 10 (9), e0138310. https://doi.org/10.1371/journal.pone.0138310.
Ouyang, X., Lin, B., 2017. Carbon dioxide (CO2) emissions during urbanization: a comparative study between China and Japan. J. Clean. Prod. 143, 356–368. https://doi.org/10.1016/j.jclepro.2016.12.102.
Ouyang, Z.T., Fan, P.L., Chen, J.Q., 2016. Urban built-up areas in transitional economies of southeast Asia: spatial extent and dynamics. Rem. Sens. 8 (10), 19. https://doi.org/10.3390/rs8100819.
Ozokcu, S., Ozdemir, O., 2017. Economic growth, energy, and environmental Kuznets curve. Renew. Sustain. Energy Rev. 72, 639–647. https://doi.org/10.1016/j.rser.2017.01.059.
Pazienza, P., 2014. The relationship between FDI and the natural environment. Contact Dermatitis 31 (5), 288–290. https://doi.org/10.1007/978-3-319-04301-2.
Riti, J.S., Song, D., Shu, Y., Kamah, M., 2017. Decoupling CO2 emission and economic growth in China: is there consistency in estimation results in analyzing environmental Kuznets curve? J. Clean. Prod. 166, 1448–1461. https://doi.org/10.1016/j.jclepro.2017.08.117.
Rosa, E.A., 2003. STIRPAT, IPAT and ImPACT: analytic tools for unpacking the driving forces of environmental impacts. Ecol. Econ. 46 (3), 351–365. https://doi.org/10.1016/S0921-8009(03)00188-5.
Rupasingha, A., Goetz, S.J., Debertin, D.L., Pagoulatos, A., 2010. The environmental Kuznets curve for US counties: a spatial econometric analysis with extensions. Pap. Reg. Sci. 83 (2), 407–424. https://doi.org/10.1007/s10110-004-0199-x.
Shan, Y., Guan, D., Hubacek, K., Zheng, B., Davis, S.J., Jia, L., Liu, J., Liu, Z., Fromer, N., Mi, Z., Meng, J., Deng, X., Li, Y., Lin, J., Schroeder, H., Weisz, H., Schellnhuber, H.J., 2018. City-level climate change mitigation in China. Science Advances 4 (6), eaaq0390. https://doi.org/10.1126/sciadv.aaq0390.
Shan, Y., Liu, J., Liu, Z., Xu, X., Shao, S., Wang, P., Guan, D., 2016. New provincial CO_2 emission inventories in China based on apparent energy consumption data and updated emission factors. Appl. Energy 184, 742–750. https://doi.org/10.1016/j.apenergy.2016.03.073.
Shao, L., Guan, D., Zhang, N., Shan, Y., Chen, G.Q., 2016. Carbon emissions from fossil fuel consumption of Beijing in 2012. Environ. Res. Lett. 11 (11), 12. https://doi.org/10.1088/1748-9326/11/11/114028.
Shen, L., Liu, L., Gao, T., Xue, J., Chen, F., 2012. The quantity, flow and functional zoning of energy resources in China. Resour. Sci. 34 (9), 1611–1621 (in Chinese).
Shi, K., Chen, Y., Yu, B., Xu, T., Chen, Z., Liu, R., Li, L., Wu, J., 2016. Modeling spatiotemporal CO2 (carbon dioxide) emission dynamics in China from DMSP-OLS nighttime stable light data using panel data analysis. Appl. Energy 168, 523–533. https://doi.org/10.1016/j.apenergy.2015.11.055.
Wang, F., Zhou, X., 2012. Impact factors of China's carbon dioxide emissions: provincial panel data analysis. Chin. J. Popul. Sci. (2), 47–56 (in Chinese).
Wang, P., Wu, W., Zhu, B., Wei, Y., 2013. Examining the impact factors of energy-related CO2 emissions using the STIRPAT model in Guangdong Province, China. Appl. Energy 106 (11), 65–71. https://doi.org/10.1016/j.apenergy.2013.01.036.
Wang, S., Fang, C., Guan, X., Pang, B., Ma, H., 2014. Urbanisation, energy consumption, and carbon dioxide emissions in China: a panel data analysis of China's provinces. Appl. Energy 136, 738–749. https://doi.org/10.1016/j.apenergy.2014.09.059.
Wang, S., Liu, X., 2017. China's city-level energy-related CO_2 emissions: spatiotemporal patterns and driving forces. Appl. Energy 200, 204–214. https://doi.org/10.1016/j.apenergy.2017.05.085.
Wang, S., Liu, X., Zhou, C., Hu, J., Ou, J., 2017. Examining the impacts of socioeconomic factors, urban form, and transportation networks on CO2 emissions in China's megacities. Appl. Energy 185, 189–200. https://doi.org/10.1016/j.apenergy.2016.10.052.
Wang, S., Su, Y., Zhao, Y., 2018. Regional inequality, spatial spillover effects and influencing factors of China's city-level energy-related carbon emissions. Acta Geograph. Sin. 73 (3), 414–428. https://doi.org/10.11821/dlxb201803003.

Wang, S., Huang, Y., 2019. Spatial spillover effect and driving forces of carbon emission intensity at city level in China. Acta Geograph. Sin. 74 (6), 1131–1148. https://doi.org/10.11821/dlxb201906005.

Wang, X., Mendelsohn, R., 2003. An economic analysis of using crop residues for energy in China. Environ. Dev. Econ. 8 (3), 467–480. https://doi.org/10.1017/s1355770x0300251.

Wang, Y., Li, G., 2016. Mapping urban CO_2 emissions using DMSP/OLS 'city lights' satellite data in China. Environ. Plann.: Economy and Space 49 (2), 248–251. https://doi.org/10.1177/0308518x16656374.

Wang, Z., Ye, X., 2017. Re-examining environmental Kuznets curve for China's city-level carbon dioxide (CO_2) emissions. Spatial Statistics 21, 377–389. https://doi.org/10.1016/j.spasta.2016.09.005.

Wu, R., Yang, D., Dong, J., Zhang, L., Xia, F., 2018a. Regional inequality in China based on NPP-VIIRS night-time light imagery. Rem. Sens. 10 (2) https://doi.org/10.3390/rs10020240.

Wu, R., Dong, J., Zhou, L., Zhang, L., 2018b. Regional distribution of carbon intensity and its driving factors in China: an empirical study based on provincial data. Pol. J. Environ. Stud. 27 (3), 1331–1341. https://doi.org/10.15244/pjoes/76364.

Xu, X.L., 2017. China population spatial distribution kilometer grid dataset. Data registration and publishing system of Resource and Environmental Science Data Center of the Chinese Academy of Sciences. https://doi.org/10.12078/2017121101. Available online: http://www.resdc.cn/DOI, 2017.

Xu, Q., Dong, Y.x., Yang, R., 2018. Urbanization impact on carbon emissions in the Pearl River Delta region: Kuznets curve relationships. J. Clean. Prod. 180, 514–523. https://doi.org/10.1016/j.jclepro.2018.01.194.

Yang, H., Flower, R.J., Thompson, J.R., 2013. Pollution: China's new leaders offer green hope. Nature 493 (7431), 163. https://doi.org/10.1038/493163d.

Yao, C., Feng, K., Hubacek, K., 2015. Driving forces of CO_2 emissions in the G20 countries: an index decomposition analysis from 1971 to 2010. Ecol. Inf. 26, 93–100. https://doi.org/10.1016/j.ecoinf.2014.02.003. Part 1, Sp. Iss. SI.

Yi, K., Tani, H., Li, Q., Zhang, J., Guo, M., Bao, Y., Wang, X., Li, J., 2014. Mapping and evaluating the urbanization process in northeast China using DMSP/OLS nighttime light data. Sensors 14 (2), 3207–3226. https://doi.org/10.3390/s140203207.

Zhang, L., Pang, J., Chen, X., Lu, Z., 2019. Carbon emissions, energy consumption and economic growth: evidence from the agricultural sector of China's main grain-producing areas. Sci. Total Environ. 665, 1017–1025. https://doi.org/10.1016/j.scitotenv.2019.02.162.

Zhang, L., Zhang, H., Yang, H., 2018. Spatial distribution pattern of the headquarters of listed firms in China. Sustainability 10 (7), 20. https://doi.org/10.3390/su10072564.

Zhang, L.F., 2012. Research of the relation between the industry structure and carbon emissions in China. Adv. Mater. Res. 485, 280–282. https://doi.org/10.4028/www.scientific.net/AMR.485.280.

Zhang, X., Wu, J., Peng, J., Cao, Q., 2017. The uncertainty of nighttime light data in estimating carbon dioxide emissions in China: a comparison between DMSP-OLS and NPP-VIIRS. Rem. Sens. 9 (8) https://doi.org/10.3390/rs9080797.

Zhao, Y., Wang, S., Zhou, C., 2016. Understanding the relation between urbanization and the eco-environment in China's Yangtze River Delta using an improved EKC model and coupling analysis. Sci. Total Environ. 571, 862–875. https://doi.org/10.1016/j.scitotenv.2016.07.067.

Zhou, C., Wang, S., 2018. Examining the determinants and the spatial nexus of city-level CO2 emissions in China: a dynamic spatial panel analysis of China's cities. J. Clean. Prod. 171, 917–926. https://doi.org/10.1016/j.jclepro.2017.10.096.

Zhou, L., Dang, X., Sun, Q., Wang, S., 2020. Multi-scenario simulation of urban land change in Shanghai by random forest and CA-Markov model. Sustainable Cities and Society 55. https://doi.org/10.1016/j.scs.2020.102045.

Zhu, Q., Peng, X., Wu, K., 2012. Calculation and decomposition of indirect carbon emissions from residential consumption in China based on the input–output model. Energy Pol. 48 (3), 618–626. https://doi.org/10.1016/j.enpol.2012.05.068.